# Supplementary material

## Materials & Methods

### General methods and buffers

Restriction enzyme digests, DNA ligations and other recombinant DNA procedures were performed using standard protocols. All mutagenesis was performed using the Quick-Change site-directed mutagenesis method (Stratagene) with the KOD polymerase (Novagen). DNA constructs used for transfection were purified from *E. coli* DH5$\alpha$ using Qiagen Plasmid kits according to the manufacturers protocol. All DNA constructs were verified by DNA sequencing.

Lysis buffer used for HEK 293 cells was 50 mM Tris-HCl pH 7.5, 1 mM EGTA, 1 mM EDTA, 1% (w/v) Nonidet P-40 (substitute), 1 mM sodium orthovanadate, 50 mM sodium fluoride, 5 mM sodium pyrophosphate, 0.27 M sucrose, 0.1% (v/v) 2-mercaptoethanol, 1 mM benzamidine, and 0.1 mM PMSF. Buffer A was 50 mM Tris-HCl pH 7.5, 0.1 mM EGTA, and 0.1% (v/v) 2-mercaptoethanol. SDS sample buffer contained 50 mM Tris-HCl pH 6.8, 2% (w/v) SDS, 10% (v/v) glycerol, 0.005% (w/v) bromophenol blue, and 1% (v/v) 2-mercaptoethanol. TBS-T buffer was Tris-HCl pH 7.5, 0.15 M NaCl, and 0.5% (v/v) Tween. All protein concentrations were determined using the Bradford reagent (Bio-Rad) and measuring the absorbance at 595 nm.

### Cloning, protein expression and purification

The MultiBac expression system (1) was used to co-produce the LKB1-STRAD$\alpha$-MO25$\alpha$ complex in *Spodoptera frugiperda* (Sf) insect cells. Expression vectors were kindly provided by Prof. Tim J. Richmond and Dr. Imre Berger (ETH Zürich, Switzerland) and the cloning procedure was followed as described previously (1). MO25$\alpha$ (residues 1-341) and STRAD$\alpha$ (residues 59-431) clones were inserted into the multiple cloning site (MCS) 1 and MSC2 of a pFBDM$^{STRAD\alpha/MO25\alpha}$ vector respectively, using EcoR1/Not1 (STRAD$\alpha$) and Xho1/Sph1 (MO25$\alpha$) restriction sites. LKB1 (residues 43-346) preceded by an N-terminal 6-His tag and a TEV protease site (sequence MAHHHHHHENLYFQG) was inserted separately into MSC2 of a different pFBDM$^{LKB1}$ vector using EcoRI/EcoRI sites. Both MSC1 and MSC2 (containg the LKB1 insert) of the pFBDM$^{LKB1}$ vector were then cut using Pme1/Avr2 restriction enzymes. This was ligated into the BstZ171/Spe1 digested pFBDM$^{STRAD\alpha/MO25\alpha}$

(containing STRAD$\alpha$/MO25$\alpha$) vector thus, generating a hybrid pFBDM vector containing all three genes. Recombinant bacmid was generated in DH10Bac$^{TM}$ cells (Invitrogen) and extracted using the phenol:chloroform method. Sf9 and Sf21 cells (Invitrogen) were cultured in Sf-900 II media following the supplier's manual. Recombinant progeny 1 (P1) baculovirus was produced by transfecting 5 ml Sf9 cells ($1.0 \times 10^6$ cells/ml), grown in 25 cm$^3$ flasks, harvested after 6 days, aliquoted and stored at -80 $^o$C. The P2 virus was generated by infecting Sf21 cells ($1.0 \times 10^6$ cells/ml) using the P1 virus (400 $\mu$l/100 ml cells). The supernatant from this culture (P2) was harvested 72 h post-infection, and 3 ml were used to infect 600 ml of Sf21 cells ($1.5 \times 10^6$ cells/ml), thus generating a P3 virus 48 h post-infection. This culture was used (1:10) to infect 6 l of Sf21 cells for protein production. Cells were grown in suspension for 48 h and the cell pellets were washed in MBS buffer (20 mM Mes/NaOH pH 6.3, 140 mM NaCl, 40 mM KCl) prior to harvesting in ice-cold lysis buffer (50 mM Tris-HCl pH 7.8, 150 mM NaCl, 5% glycerol, 0.2 mM EDTA, 0.2 mM EGTA, 1 mM benzamidine, 0.2 mM PMSF, 5 $\mu$M leupeptine, 20 mM imidazole and 0.075% (v/v) $\beta$-mercaptoethanol). Cells were lysed using a continuous flow cell disruptor at 35000 psi, and the lysate was clarified by centrifugation at 26000 g for 30 min. The supernatant was incubated on a rolling platform for 1 h at 4$^o$C with 8 ml of NiNTA agarose beads (Qiagen), pre-equilibrated in low salt buffer (50 mM Tris-HCl pH 7.8, 150 mM NaCl, 5% (v/v) glycerol, 0.2 mM EDTA, 0.2 mM EGTA, 1 mM benzamidine, 20 mM imidazole and 0.075% (v/v) $\beta$-mercaptoethanol). The beads were washed with 10 column volumes (CV) of low salt buffer and 60 CV of high salt buffer (low salt buffer containing 500 mM NaCl), followed by 10 CV of low salt buffer. The protein was eluted from a disposable column with 10 CV of low salt buffer supplemented with 100 mM imidazole. Fractions were pooled (60 mg of protein) and 3 mg of His tagged TEV protease was added prior to dialyses against 5 l of low salt buffer (containing 50 mM NaCl) for 48 h. The TEV protease and uncleaved LKB1 were removed by passing through 2 ml of NiNTA beads prior to loading the sample on a 5 ml HiTrap-Q column (GE Healthcare). Bound proteins were eluted over 30 CV using a salt gradient of 0-500 mM NaCl and the LKB1-STRAD$\alpha$-MO25$\alpha$ complex eluted as a single peak at $\sim$250 mM NaCl. The sample was divided in half, concentrated to 3 ml and loaded on a Sepharose-S200 26/60 column (GE Healthcare), pre-equilibrated in 25 mM Tris-HCl pH 7.8, 350 mM NaCl and 2 mM TCEP. Alternatively the protein sample was methylated using the protocol described elsewhere (2; 3) before loading on a gel filtration column as described above. In both occasions the LKB1-STRAD$\alpha$-MO25$\alpha$ complex eluted as a single peak and its purity was assessed by SDS-PAGE

and MALDI-TOF linear mass spectrometry.

### Crystallization, structure solution and refinement

Both methylated and unmethylated LKB1-STRAD$\alpha$-MO25$\alpha$ complex were concentrated to 8.0 mg/ml followed by the addition of AMP-PNP and $MgCl_2$ to a final concentration of 5 mM. Crystals were grown at 20 $^o$C using the hanging drop vapour diffusion method. Crystals of the unmethylated sample were obtained by mixing 1.5 $\mu$l of protein and 1.2 $\mu$l of mother liquor (1.8 M $(NH_4)_2SO_4$, 0.1 M Tris-HCl pH 9.0) and 0.3 $\mu$l of 2 mM NaCl. For the methylated protein sample, crystals were grown by mixing 1.5 $\mu$l of protein with 1.5 $\mu$l of mother liquor (1.6 M $(NH_4)_2SO_4$, 0.1 M Tris-HCl pH 8.25). In both cases crystals appeared after 36-48 h and reached maximal size after 4 days.

Data were collected at 100 K on station ID14-3 at the European Synchrotron Radiation Facility (ESRF) and processed using the DENZO and SCALEPACK programs from the HKL2000 suite (4) (Table S1).

The structures of the unmethylated/methylated complexes were solved by a combination of molecular replacement with PHASER (5) and averaging/automatic model building using RESOLVE (6). A molecular replacement run was carried out using the structures of MO25$\alpha$ (PDBID 1UPK (7)) and STRAD$\alpha$ (PDBID 3GNI (3)) as search models. This gave a solution with two copies of each model in the asymmetric unit (asu). The resulting model phases were then further improved by solvent flattening and two-fold averaging using RESOLVE (6), which also built four LKB1 fragments as C$\alpha$ trace. Using the partially built LKB1 model, the structure of the AUR2 protein kinase (PDBID 1OL7 (8), 24.5% sequence identity to LKB1) was superimposed using the secondary structure matching function in COOT (9). Regions of this initial LKB1 model that did not have any associated electron density were removed. The structure was further refined by alternating rounds of refinement with PHENIX (10) and REFMAC (11) (using strict NCS during the first macrocycles and TLS refinement during the last macrocycles) and manual model building with the program COOT (9). For the methylated complex, this resulted in a final model consisting of 1835 ordered residues out of 2080 possible residues, with an R-factor of 0.239 ($R_{free} = 0.290$, Supplementary Table I), that was validated using PROCHECK (12) and MOLPROBITY (13).

Figures were prepared using the PyMOL molecular graphics system available at http://www.pymol.org (14). Secondary structure was analysed using DSSP (15) and sequence alignments were performed using MUSCLE (16), which were edited and displayed using the program ALINE

(17).

### Cell culture, transfections and lysis

293 cells were cultured on 10 cm diameter dishes in 10 ml DMEM supplemented with 10% (v/v) fetal bovine serum, 2 mM L-glutamine, 100 U/ml penicillin, and 0.1 mg/ml streptomycin. For transfection experiments, 3 to 9 $\mu$g of DNA was mixed with 20 $\mu$l of 1 mg/ml polyethylenimine (Polysciences) in 1 ml of plain DMEM for each dish, and the mixture was left to stand for 30 min and added onto the cells. Cells were lysed 36 hours post-transfection in 1 ml of ice-cold lysis buffer per dish. The cell lysates were clarified by centrifugation at 20,000 g for 15 min at 4 $^o$C, and the supernatants divided into aliquots, frozen in liquid nitrogen and stored at -20 $^o$C.

### Expression of fusion proteins in HEK293 cells and affinity purification

10 cm diameter dishes of 293 cells were transiently transfected with 3 $\mu$g of the pEBG-2T constructs (GST-LKB1) together with 3 $\mu$g of the indicated pCMV5 constructs (Flag-STRAD$\alpha$ and Myc-MO25$\alpha$). Cells were harvested and lysed 36 h post-transfection and the clarified lysates were incubated for 1 h on a rotating platform with glutathione-Sepharose (GE Healthcare; 20 $\mu$l/dish of lysate) previously equilibrated in lysis buffer. The beads were washed twice with lysis buffer containing 150 mM NaCl and twice with 50 mM Tris-HCl, pH 7.5 For immunoblotting analysis, the beads were then resuspended in SDS sample buffer after this step and the samples immunoblotted as described above. For protein kinase assays and gel electrophoresis, the beads were washed twice with buffer A, and the proteins were eluted from the resin by incubation with the same buffer containing 20 mM reduced glutathione and 270 mM sucrose. The beads were then removed by filtration through a 0.44 $\mu$m filter and the eluate was divided into aliquots and stored at -80 $^o$C.

### Assaying LKB1 by measuring phosphorylation of the LKBtide peptide

The activity of recombinant LKB1-STRAD$\alpha$-MO25$\alpha$ complexes was assayed towards the LKBtide peptide substrate (SNLYHQGKFLQTFCGSPLYRRR) (18). All assays were performed by using 0.35 $\mu$g of recombinant proteins expressed and purified from HEK293 cells as described above. Phosphotransferase activity towards the LKBtide peptide was measured in a total assay volume of 50 $\mu$l consisting of 50 mM Tris-HCl, pH 7.5, 0.1 mM EGTA, 0.1% (v/v) 2-mercaptoethanol, 10 mM magnesium acetate, 0.1 mM [$\gamma$-$^{32}$P]ATP (200 cpm/pmol)

and 0.2 mM LKBtide peptide. The assays were carried out at 30 $^{o}$C and were terminated after 15 minutes by applying 40 $\mu$l of the reaction mixture onto P81 membranes. These were washed in phosphoric acid, and the incorporated radioactivity was measured by scintillation counting as described previously for MAP kinase (19). One Unit (U) of activity represents the incorporation to the substrate of 1 nmol of $\gamma$-$^{32}$P per minute.

### Assaying LKB1 by measuring activation of the heterotrimeric AMPK kinase

The AMPK heterotrimeric complex was purified from *E. coli* following the protocol from Neumann *et al.*, 2003 (20) and the AMPK activity was measured following its phosphorylation with LKB1 as reported by Lizcano *et al.*, 2004 (18; 3). 0.3 $\mu$g of AMPK complex ($\alpha_1\beta_2\gamma_1$ subunits), were incubated with or without 10 ng of wild type or mutant LKB1-STRAD$\alpha$-MO25$\alpha$ complex in Buffer A containing 5 mM magnesium acetate and 0.1 mM cold ATP, in a final volume of 20 $\mu$l. After incubation at 30 $^{o}$C for 30 minutes the AMPK kinase activity was determined by adding 30 $\mu$l of Buffer A containing 5 mM magnesium acetate, 0.1 mM [$\gamma$-$^{32}$P]ATP (300 cpm/pmol) and 0.2 mM AMARA peptide (AMARAASAAALARRR) (21) as substrate. After incubation for 20 min at 30 $^{o}$C, incorporation of $\gamma$-$^{32}$P into the peptide substrate was determined by applying the reaction mixture onto P81 phosphocellulose paper and scintillation counting as described in the previous section. One Unit (U) of activity represents the incorporation to the substrate of 1 nmol of $\gamma$-$^{32}$P per minute.

### Immunoblotting

The indicated amounts of cell lysates or purified proteins were subjected to SDS-PAGE and transferred to nitrocellulose membranes. The membranes were blocked for 1 hour in TBS-T buffer containing 5% (w/v) skimmed milk. The anti-GST, anti-Flag and anti-Myc antibodies (Sigma) were diluted 1000-fold before the membranes were immunoblotted in the same buffer containing the indicated antibodies, for 16 hours at 4 $^{o}$C. Membranes were then washed six times with TBS-T buffer and incubated with the appropriate horseradish peroxidase-conjugated secondary antibodies (Pierce) in TBS-T buffer containing 10% (w/v) skimmed milk. After repeating the washing steps, detection was performed using the enhanced chemiluminescence reagent (Amersham Pharmacia Biotech) and the films were developed using a film automatic processor (SRX-101; Konica Minolta Medical).

## Supplementary figures

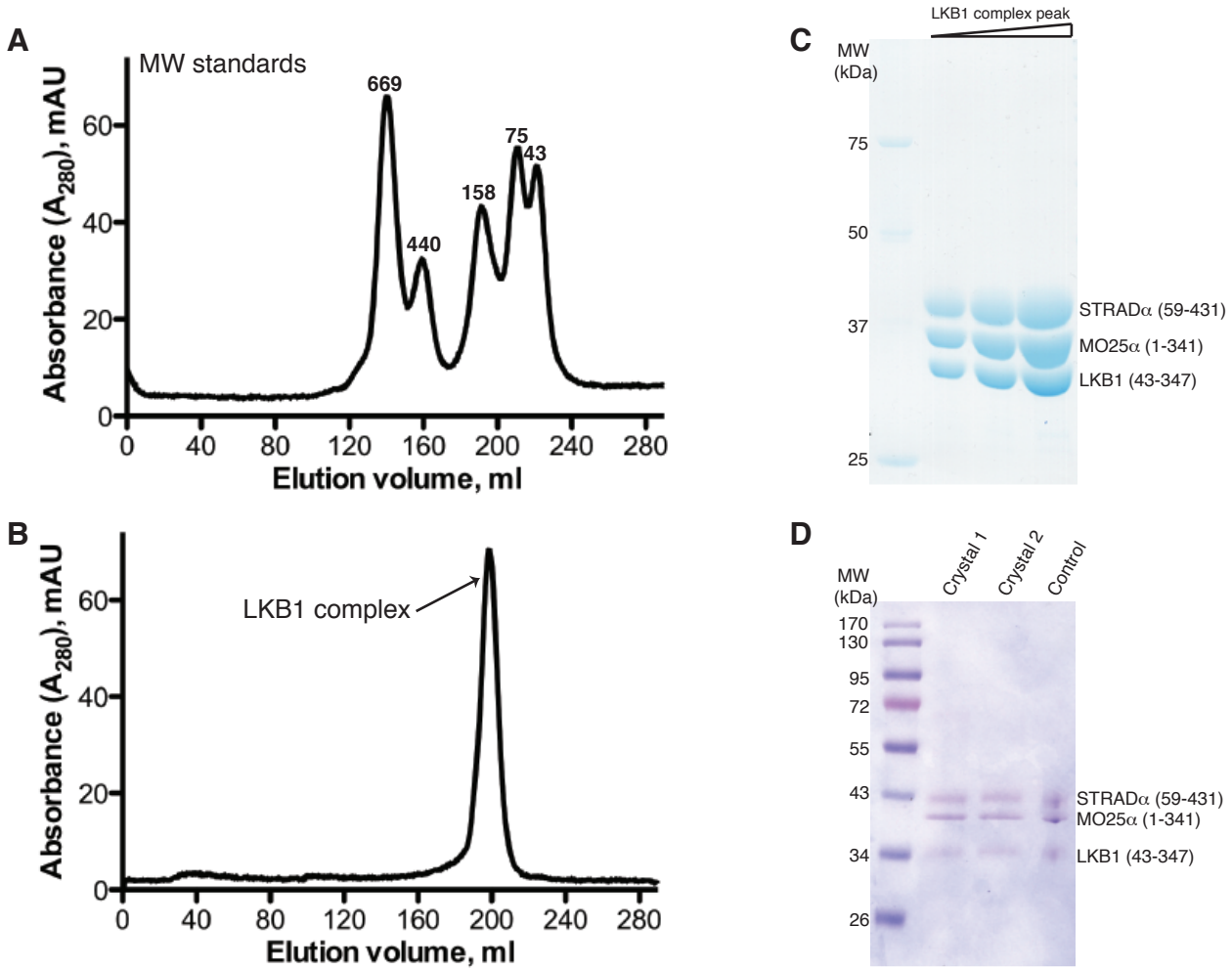


**Figure S1: Isolation of the heterotrimeric LKB1/STRAD$\alpha$/MO25$\alpha$ complex**
A) Elution profile of the molecular mass standards, Thyroglobulin (669 kDa), Ferritin (440 kDa), Aldolase (158 kDa), Conalbumin (75 kDa) and Ovalbumin (43 kDa).
B) Elution profile of the LKB1 heterotrimeric complex from a Superdex26/60 S200 column.
C) Typical SDS-PAGE gel (Coomassie stained) of the combined fractions from the LKB1 complex peak that was used for crystallization.
D) SDS-PAGE gel (Coomassie stained) of LKB1 complex crystals, after three subsequent washes in mother liquor (done in duplicate). Purified LKB1 complex was used as control.

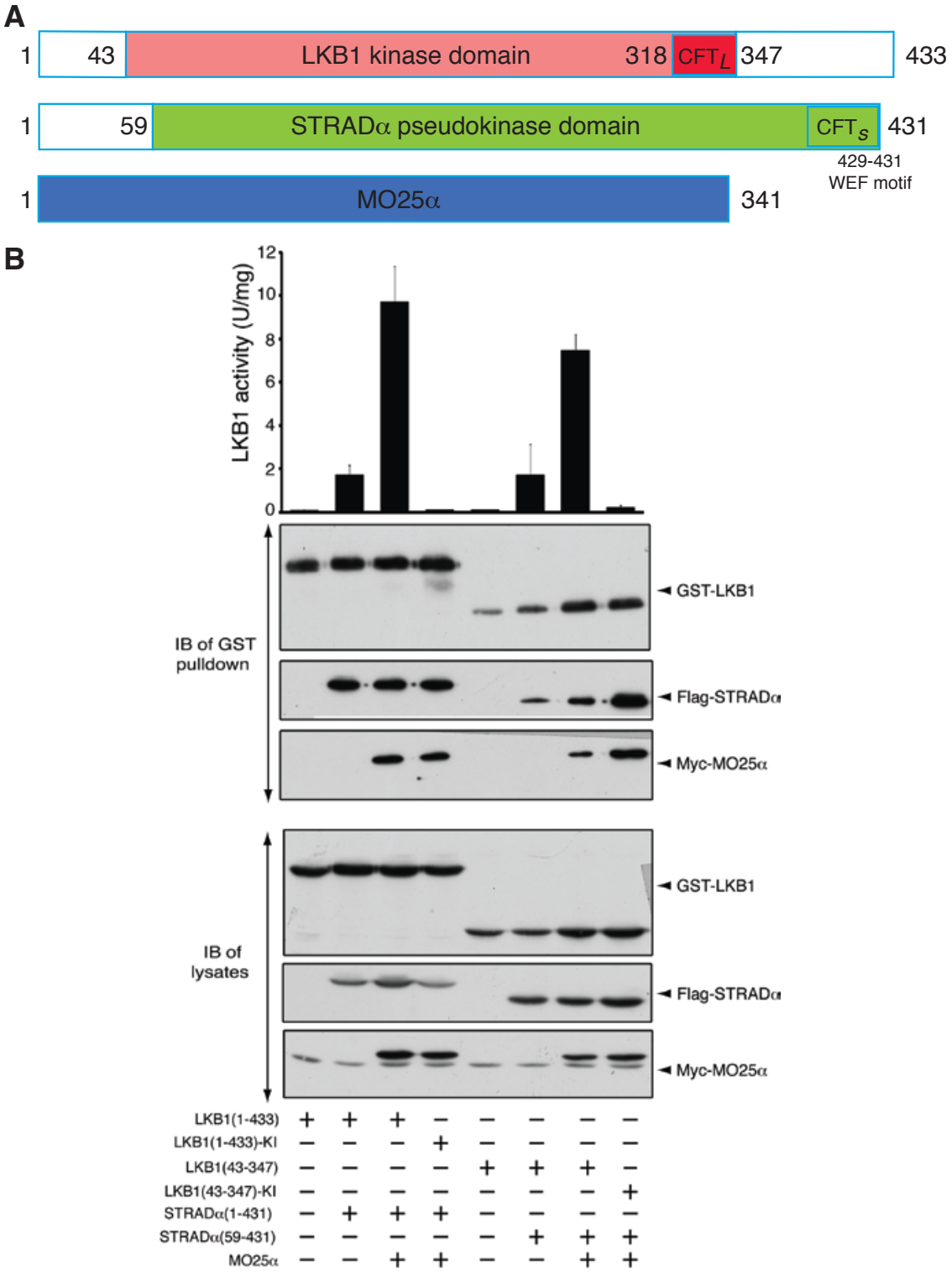


**Figure S2: Domain boundaries and activity of the core LKB1 complex**
A) Domain organization of components of the LKB1-STRAD$\alpha$-MO25$\alpha$ heterotrimer. Coloured boxes represent constructs used for crystallization. The same colouring code is used throughout this article, unless specified otherwise.
B) Activation of LKB1 by STRAD$\alpha$ and MO25$\alpha$. 293 cells were co-transfected with the indicated constructs of GST-LKB1, Flag-STRAD$\alpha$ and Myc-MO25$\alpha$. Cells at 36 h post-transfection were lysed and GST-LKB1 affinity purified and assayed for the ability to phosphorylate LKBtide as described in the Materials and Methods section (WT, wild type; KI, kinase inactive (D174A) mutant).

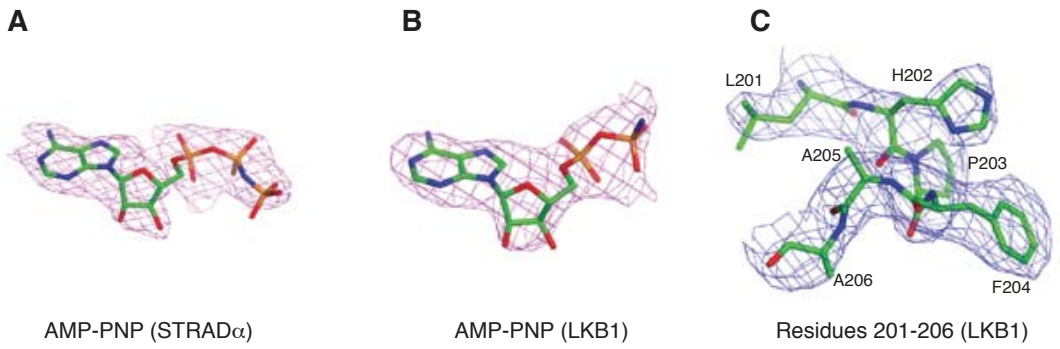


**Figure S3: Electron density maps**
A & B) Unbiased $F_o$-$F_c$ electron density maps (coloured magenta and contoured at 2.5$\sigma$), for AMP-PNP bound to STRAD$\alpha$ (A) and LKB1 (B). Density for the $\gamma$-P of AMP-PNP bound to LKB1 is lacking.
C) Final $2F_o$-$F_c$ electron density maps (coloured blue and contoured at 1$\sigma$), for the region of LKB1 activation loop that interacts with MO25$\alpha$ and shown in Fig. 1D.

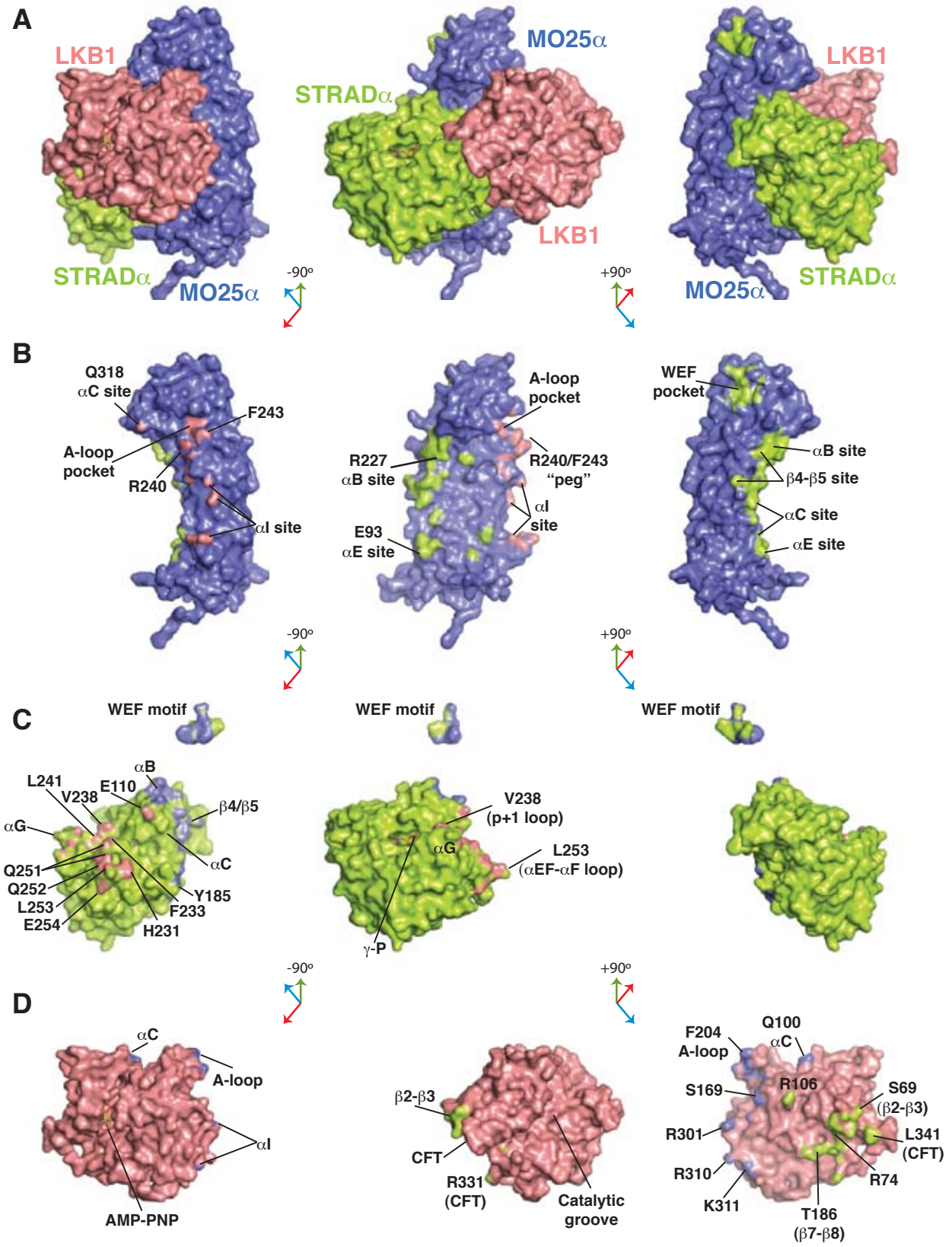


**Figure S4: Sites of the LKB1/STRADα/MO25α interaction**

A) Surface representation of the LKB1/STRADα/MO25α heterotrimer is shown at three alternative views: centre, rotated by -90 and 90$^o$ in the left and right panels respectively.

B, C & D) MO25α (blue), STRADα (green) and LKB1 (pink) are shown in the same orientations as in panel (A). A map of interaction surfaces as defined by the program CONTACT (atom pairs closer than 3.9 Å) is coloured correspondingly. Residues that are discussed further in the text are labelled to aid orientation and visualization. For a full list of interacting residues and their evolutionary conservation, see sequence alignments in Figs. S12, S11 and S10.

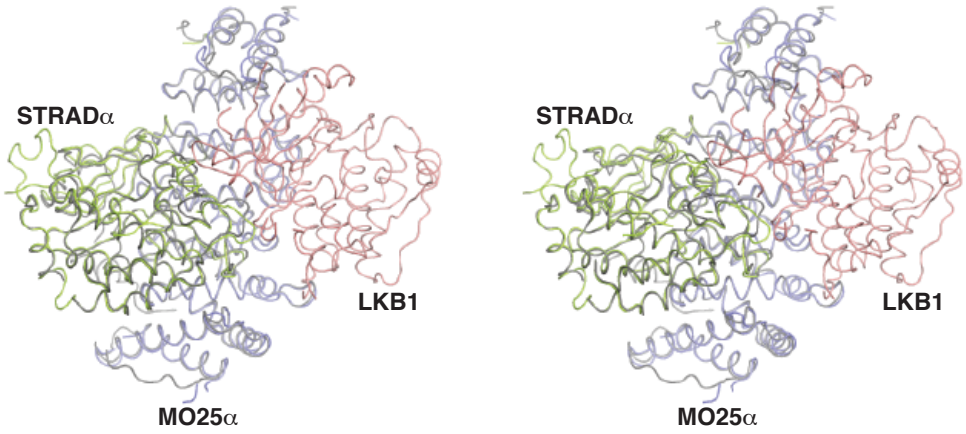


**Figure S5: Superposition of the STRADα/MO25α dimer with the LKB1 heterotrimer**
Stereo view of a superposed STRADα/MO25α complex (coloured gray, PDBID 3GNI (3)) and the LKB1/STRADα/MO25α heterotrimer. RMSD = 0.5 Å on 529 Cα atoms.

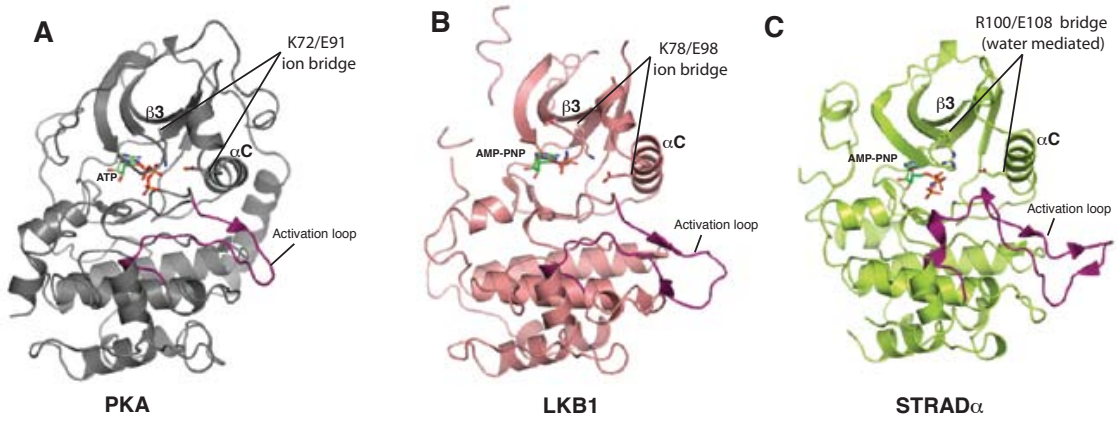


**Figure S6: Active conformations of PKA, LKB1 and STRADα**
A) Active (closed) conformation of PKA kinase domain (PDBID 1ATP) (22). The activation loop is coloured magenta and the conserved K72/E92 ion bridge (23; 24) is labelled.
B & C) Active (closed) conformations of LKB1 kinase domain (E) and STRADα "pseudokinase" domain (F) are shown in the same orientation as PKA. The activation loops are coloured magenta and the conserved K78/E98 (LKB1) and R100/E108 (STRADα) ion bridge (23; 24) are labelled.

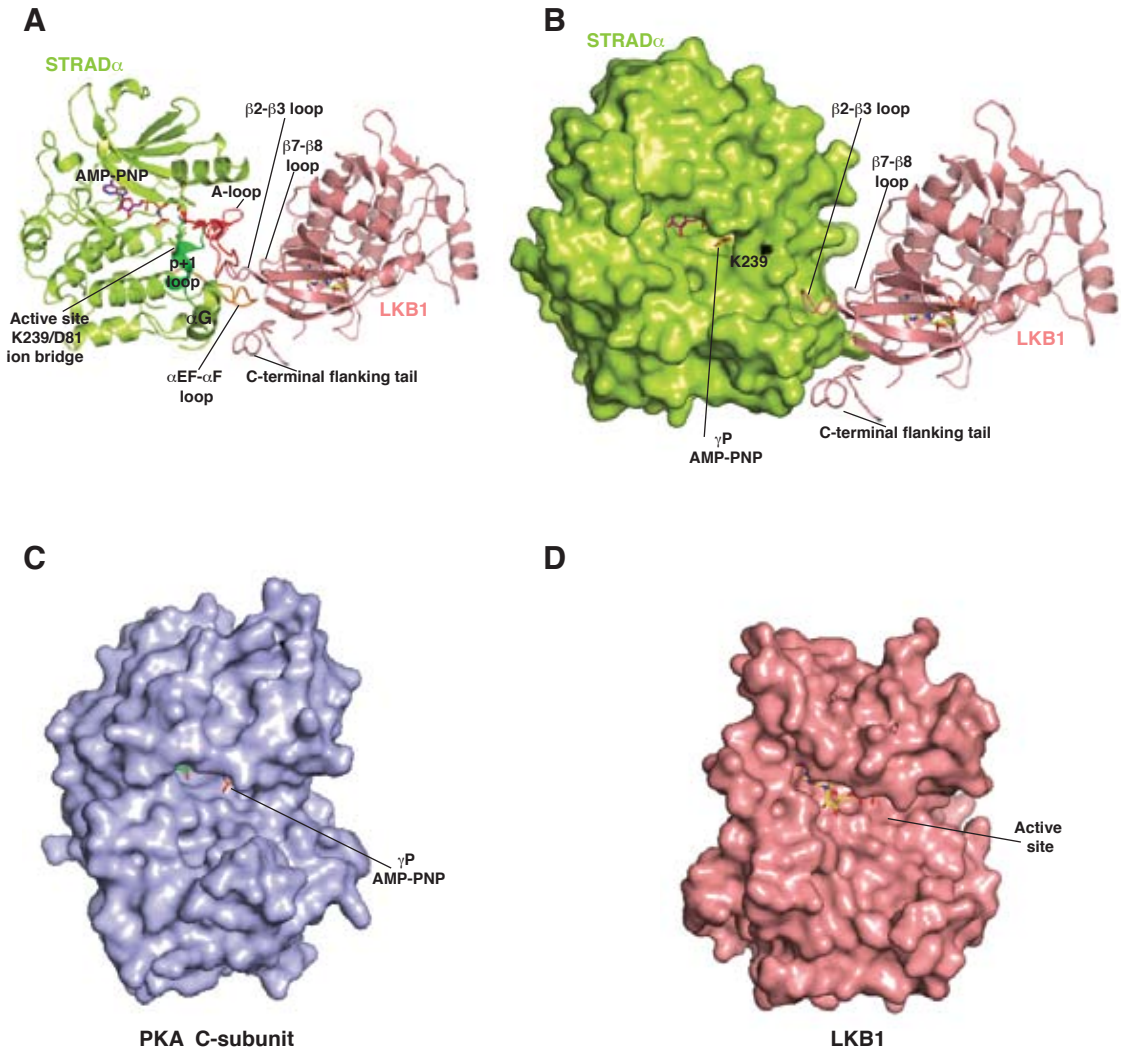


**Figure S7: STRADα/LKB1 interaction and STRADα "active site"**
A & B) Sites of STRADα/LKB1 interaction are labelled and STRADα is displayed as cartoon (A) and surface models (B). The activation loop of STRADα is coloured red and αEF-αF loop is coloured orange. STRADα K239 from the p+1 loop and D81 from β1/β2 loop are displayed as green sticks and surface. C & D ) Surface representation of structures of kinase domains of the PKA C-subunit (PDBID 2QCS (25)) and LKB1, shown in the same orientation as STRADα in panel A.

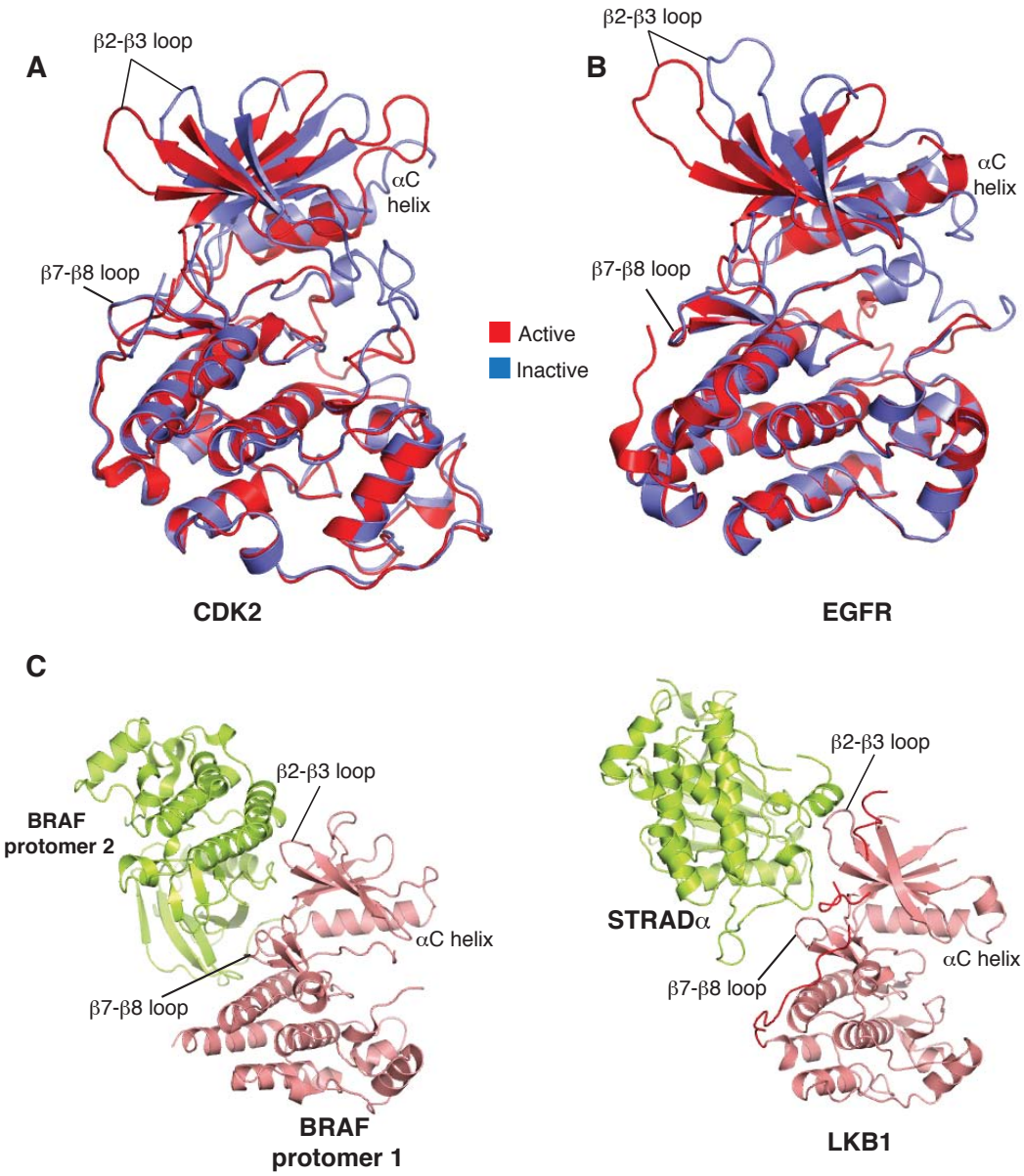


**Figure S8: Examples of kinase domains in the open and closed conformations**
A & B) Comparison of the open (blue) and closed (red) conformations of CDK2 and EGFR kinase domains. C-lobe residues from the active structures of CDK2 (PDBID 1JST (26)) and EGFR (PDBID 2GS2 (27)) were superimposed onto the structures of inactive CDK2 (PDBID 1HCK (28)) and EGFR kinase structures (PDBID 2GS7 (27)).
C) Comparison of STRAD binding to the $\beta$2-$\beta$3 loop of LKB1 with the RAF dimeric interaction (PDBID 1UWH (29)). A crystallographic contact of RAF protomer 2 via the $\beta$2-$\beta$3 and the $\alpha$C helix of protomer 1 is thought to be biologically important for BRAF activation (30).

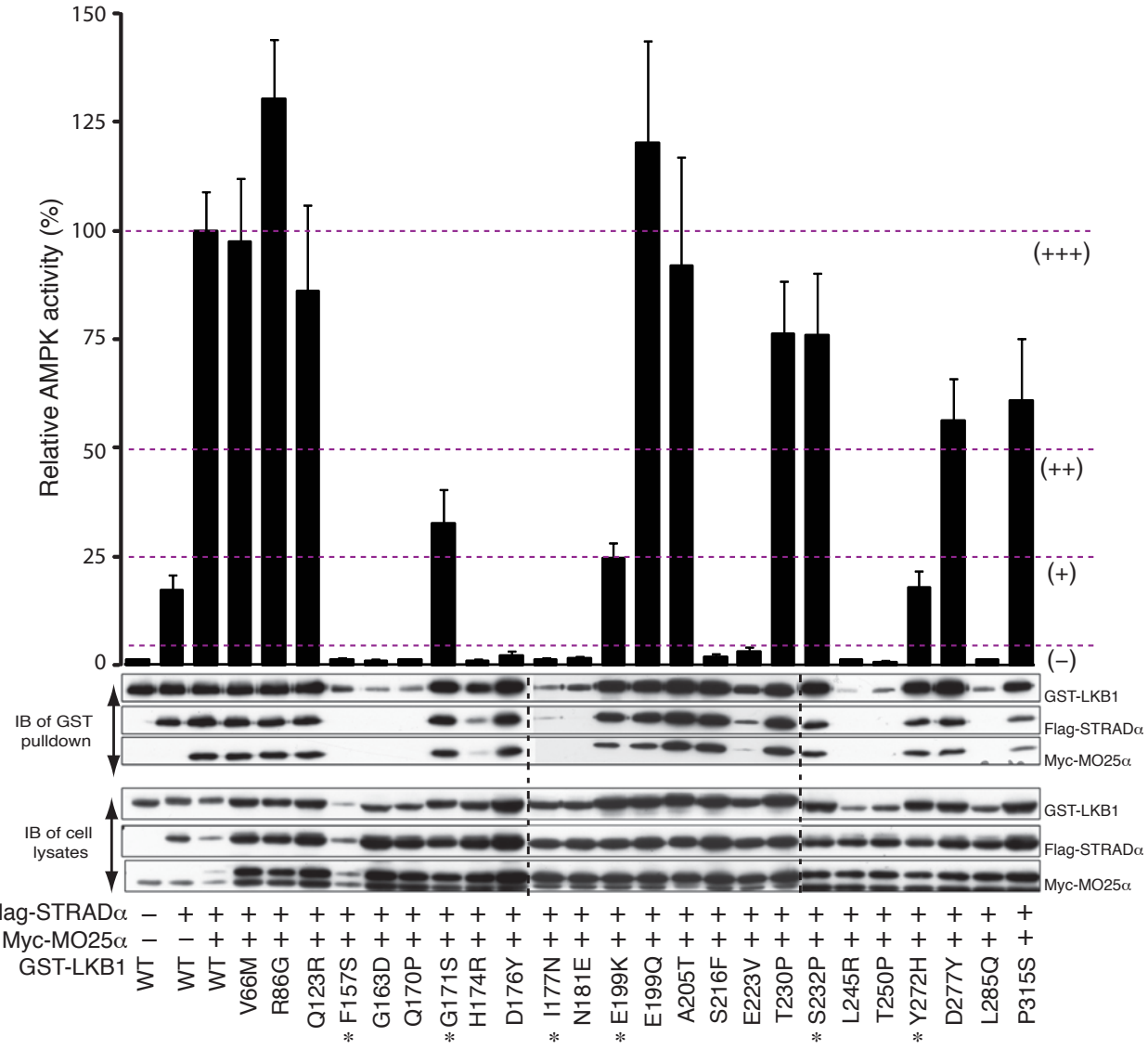


**Figure S9: Effect of the oncogenic mutations on LKB1 activity**

293 cells were co-transfected with the indicated constructs of GST-LKB1, Flag-STRAD$\alpha$ and Myc-MO25$\alpha$. Cells at 36 h post-transfection were lysed and GST-LKB1 affinity purified and assayed for the ability to activate heterotrimeric AMPK complex expressed in *E. coli* as described in the Materials and Methods section. Kinase activities are standardized relative to the activity of the wild type LKB1-STRAD$\alpha$-MO25$\alpha$ complex ($-$, $<$5%; $+$, 5-25%; $++$, 25-50%; $+++$, $>$50%) and represent the average of six independently purified complexes, assayed in duplicate (error bars represent the SEM). Representative Western blots of affinity purified GST-LKB1 preparations (upper panel) as well as cell extracts (lower panels), probed with the indicated antibodies are also shown. Asterisk indicate mutation was previously investigated by Boudeau *et al.*, (31).

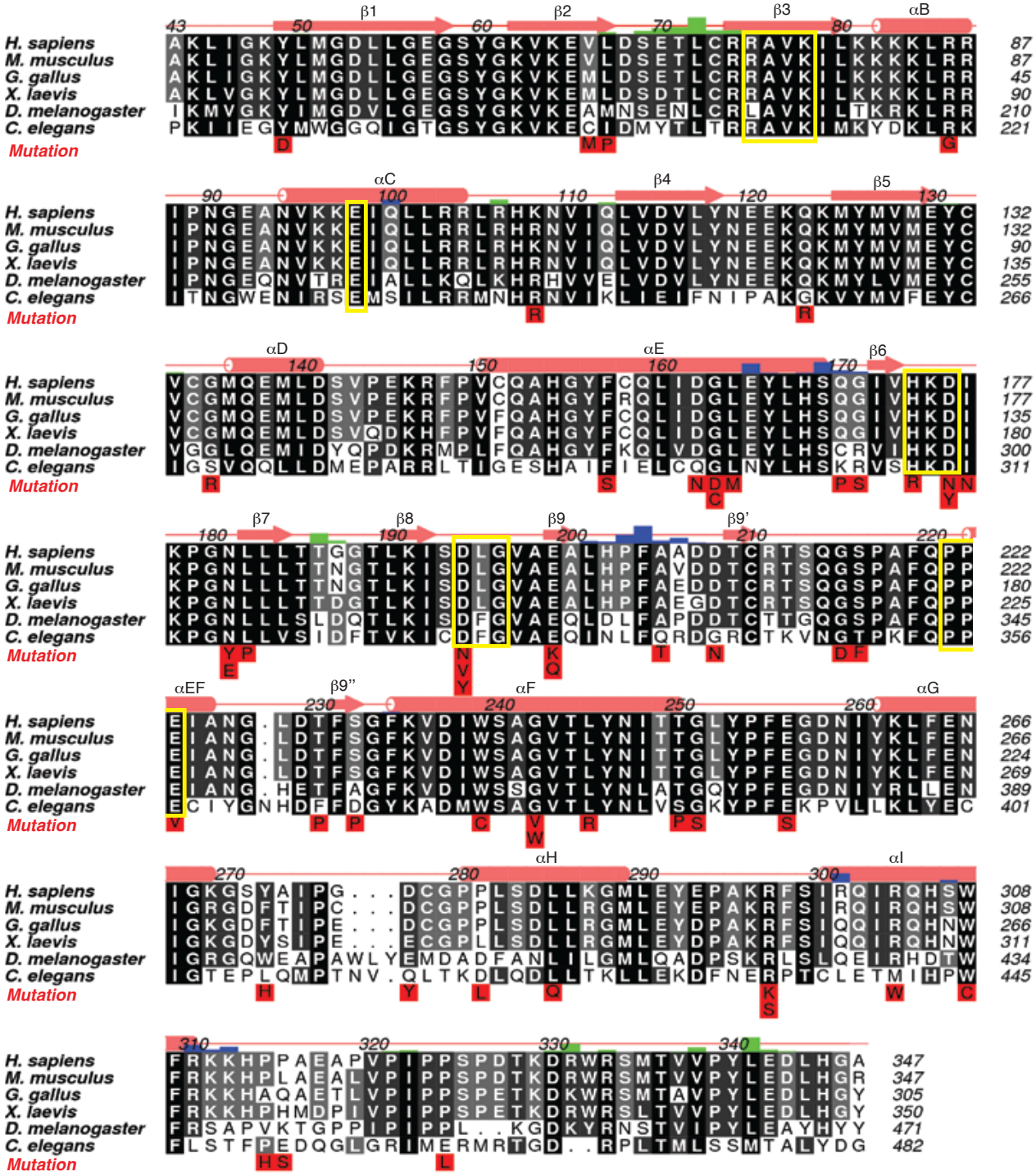


**Figure S10: LKB1 multiple sequence alignment, secondary structure and residues contributing to the interactions with STRAD$\alpha$/MO25$\alpha$**

Multiple sequence alignment (black = conserved, white = not conserved) of LKB1 from the indicated species of the metazoan kingdom. Alignments were performed with MUSCLE (16) and edited and displayed using ALINE (17). A graph of residues involved in STRAD$\alpha$/MO25$\alpha$ interaction against their contact area (green bars = STRAD$\alpha$, blue bars = MO25$\alpha$), is displayed. Height of the bar represents the contact area (atom pairs closer than 3.9 Å, analysed by CONTACT from the CCP4 package (32)), divided by the total surface area of the participating amino acid. Key LKB1 catalytic motifs are boxed. The secondary structure (analysed by DSSP (15)) is shown in pink. Disease-causing mutations are displayed at the corresponding amino acid position and have been coloured red.

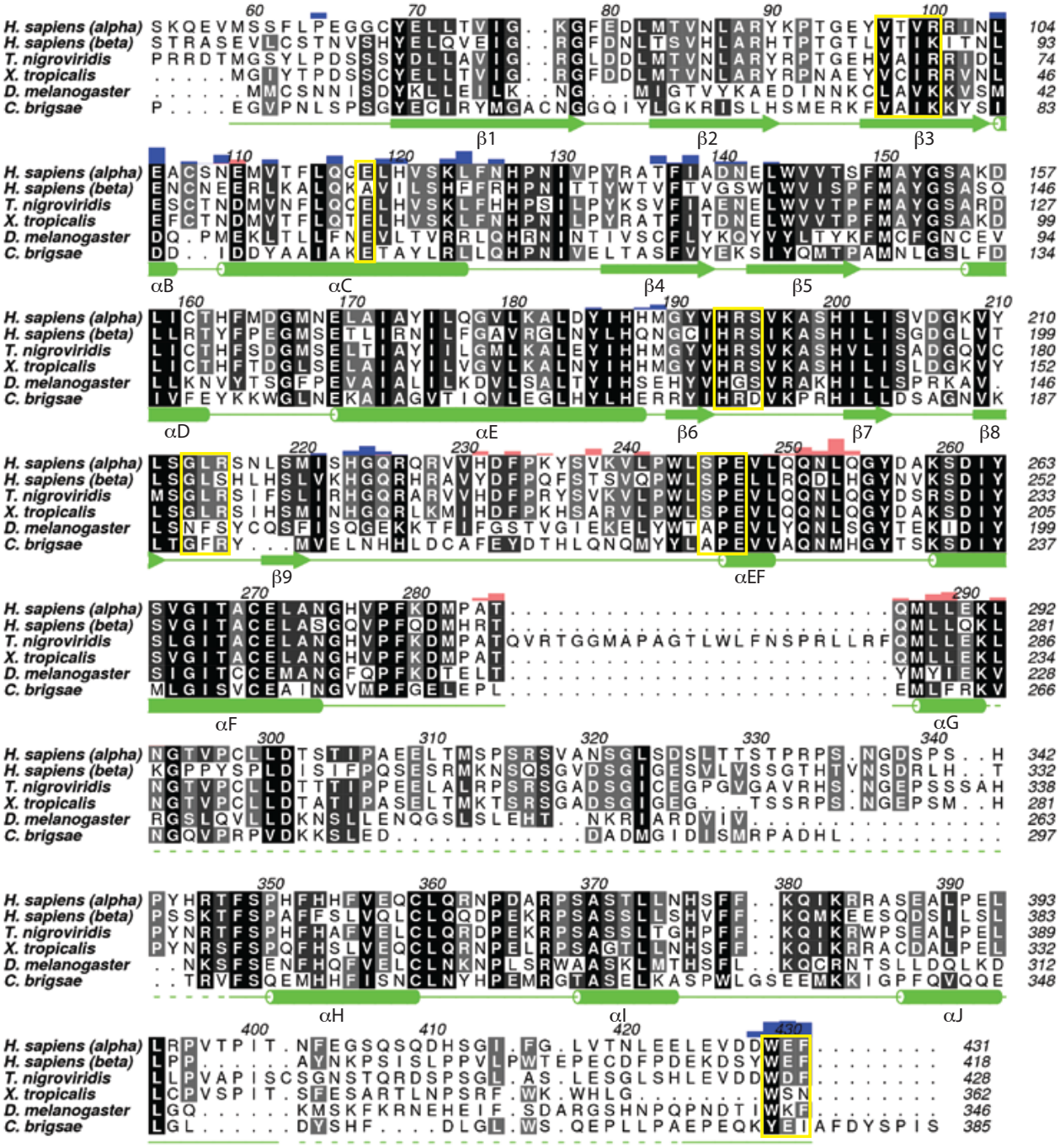


**Figure S11: STRAD$\alpha$ multiple sequence alignment, secondary structure and residues contributing to the interactions with LKB1/MO25$\alpha$**

Multiple sequence alignment (black = conserved, white = not conserved) of STRAD$\alpha$ from the indicated species of the metazoan kingdom. Alignments were performed with MUSCLE (16) and edited and displayed using ALINE (17). A graph of residues involved in LKB1/MO25$\alpha$ interaction against their contact area (blue bars = MO25$\alpha$, pink bars = LKB1), is displayed. Height of the bar represents the contact area (atom pairs closer than 3.9 Å, analysed by CONTACT from the CCP4 package (32)), divided by the total surface area of the participating amino acid. Key STRAD$\alpha$ "catalytic" motifs and the WEF motif are boxed. The secondary structure (analysed by DSSP (15)) is shown in green.

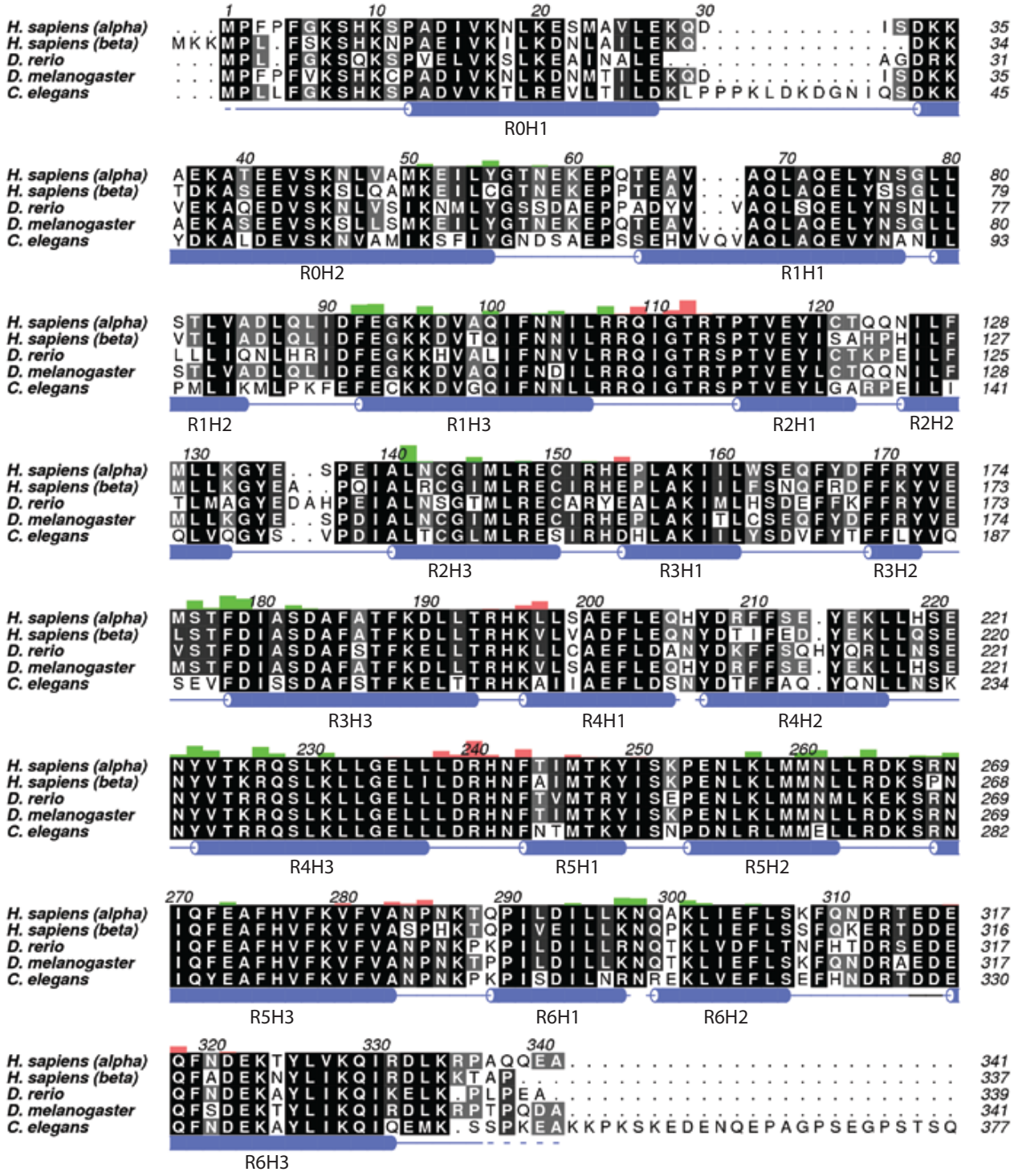


**Figure S12: MO25$\alpha$ multiple sequence alignment, secondary structure and residues contributing to the interactions with LKB1/STRAD$\alpha$**

Multiple sequence alignment (black = conserved, white = not conserved) of MO25$\alpha$ from the indicated species of the metazoan kingdom. Alignments were performed with MUSCLE (16) and edited and displayed using ALINE (17). A graph of residues involved in LKB1/STRAD$\alpha$ interaction against their contact area (green bars = STRAD$\alpha$, pink bars = LKB1) is displayed. Height of the bar represents the contact area (atom pairs closer than 3.9 Å, analysed by CONTACT from the CCP4 package (32)), divided by the total surface area of the participating amino acid. The secondary structure (analysed by DSSP (15)) is shown in red.

## Supplementary tables

**Table S1: Summary of data collection, structure refinement and analysis. Values for the highest resolution shell are given in brackets.**

| | **Native** | **Methylated** |
|---|---|---|
| Space Group | $P3_121$ | $P3_121$ |
| Unit cell (Å) | $a = 118.7$ | $a = 118.4$ |
| | $b = 118.7$ | $b = 118.4$ |
| | $c = 390.0$ | $c = 390.0$ |
| Molecules/asu | | |
| LKB1 | 2 | 2 |
| STRAD$\alpha$ | 2 | 2 |
| MO25$\alpha$ | 2 | 2 |
| Resolution (Å) | 29.0-3.0 (3.1-3.0) | 20.0-2.65 (2.75-2.65) |
| Observed reflections | 284269 | 400006 |
| Unique reflections | 61869 (6033) | 91884 (9144) |
| Redundancy | 4.6 (4.6) | 4.4 (4.4) |
| $I/\sigma I$ | 13.6 (1.6) | 14.8 (2.6) |
| Completeness (%) | 95.2 (94.6) | 99.2 (99.8) |
| $R_{merge}$ | 0.079 (0.743) | 0.063 (0.648) |
| $R_{work}$, $R_{free}$ | - | 0.239, 0.290 |
| RMSD from ideal geometry | | |
| bonds (Å) | - | 0.009 |
| angles ($^o$) | - | 1.286 |
| B-factor RMSD (Å$^2$) | | |
| (backbone bonds) | - | 0.83 |
| B (Å$^2$) | | |
| protein | - | 41.07 |
| ligands (AMP-PNP) | - | 82.52 |
| water | - | 51.50 |

**Table S2: Cancer causing mutations found in the LKB1 tumour suppressor kinase domain and the C-terminal flanking tail (33; 34; 35; 36).**

| Mutation | Disease | Location and functional significance | Comp. | Act. | Ref. |
|---|---|---|---|---|---|
| Y49D | PJS | $\beta$1, possible destabilization of the N-lobe | Yes | + | (37) |
| V66M* | PJS, Cervix | $\beta$2, possible destabilization of the N-lobe | Yes | +++ | (38) |
| L67P | PJS | $\beta$2, possible destabilization of the N-lobe | No | – | (39) |
| R86G* | PJS, NSCLC | $\alpha$B, basic (Arg-rich) region; solvent exposed | Yes | +++ | (40) |
| K108R | PJS | HKN loop | Yes | +++ | (41) |
| Q123R* | NCLS | $\beta$4-$\beta$5 loop; solvent exposed | Yes | +++ | (42) |
| G135R | PJS | Hinge region, ATP binding | Yes | – | (37) |
| F157S** | PJS | Part of hydrophobic cluster 1: L245, M289, I303, F309, L285 | No | – | (43) |
| D162N | PJS | Structural role; forms ion pair with R304 | Yes | +++ | (44) |
| G163D* | PJS, NSCLC | Presence of side chain may distort the LKB1 catalytic loop | No | – | (44) |
| L164M | PJS | Mutation may misposition the catalytic HRD motif | Yes | +++ | (44) |
| Q170P* | PJS | Structural role, possible distortion of helix $\alpha$E | No | – | (36) |
| G171S** | PJS | May interfere with the correct positioning of R240 | Yes | ++ | (45) |
| H174R* | NSCLC | Part of the catalytic HKD motif | Yes | – | (46) |
| D176N | PJS | Catalytic residue, HKD motif | Yes | – | (47) |
| D176Y* | PJS | Catalytic residue, HKD motif | Yes | – | (48) |
| I177N** | PJS | Part of hydrophobic cluster 2: L160, L164, L182 | No | – | (49) |
| N181Y | PJS | Hydrogen bonding with catalytic residue D176 and ATP | Yes | – | (43) |
| N181E* | PJS | Hydrogen bonding with catalytic residue D176 and ATP | No | – | (43) |
| L182P | PJS | Part of hydrophobic cluster 2; possible disruption of $\beta$6-$\beta$9 sheet | No | – | (41) |
| D194N/V/Y | PJS, NSCLC | $Mg^{2+}$ binding residue, catalysis | Yes | – | (44; 50; 51) |
| E199K** | PJS | Interacts with backbone atoms from LKB1 A-loop | Yes | + | (45) |
| E199Q* | PJS | Interacts with backbone atoms from LKB1 A-loop | Yes | +++ | (46) |
| A205T* | HNSCC | Possible distortion of LKB1 activation loop | Yes | +++ | (52) |
| D208N | PJS | Activation segment, interacts with the $\alpha$EF-$\alpha$F loop | Yes | +++ | (45) |
| G215D | PJS | p+1 loop, substrate binding | Yes | – | (45) |
| S216F* | PJS, NSCLC | p+1 loop, substrate binding | Yes | – | (42) |
| E223V* | NSCLC | Part of the PPE motif; forms ion pair with R297 | Yes | – | (53) |
| T230P* | PJS | Short $\beta$-strand with A-loop | Yes | +++ | (36) |
| S232P** | PJS | Short $\beta$-strand with A-loop; interacts with D208 | Yes | +++ | (54) |
| W239C | PJS | Structural role; interacts with L290 and the PPE motif | No | – | (55) |
| G242W/V | PJS | Structural role; $\alpha$H | No | – | (41) |
| L245R* | PJS | Structural role; Possible clashes with W308, L282 | No | – | (36) |
| T250P* | NSCLC | Structural role; C-terminal of helix $\alpha$F | No | – | (53) |
| G251S | PJS | Possible distortion of the hinge region | Yes | +++ | (56) |
| E256S | PJS, NSCLC | Solvent exposed. Binding of possible interactors/substrates | Yes | +++ | (54) |
| Y272H** | PJS | $\alpha$G-$\alpha$H loop. Solvent exposed | Yes | + | (57) |
| D277Y* | PJS, NSCLC | $\alpha$G-$\alpha$H loop. Solvent exposed | Yes | +++ | (48) |
| P281L | PJS | Provides turn between $\alpha$G-$\alpha$H loop into $\alpha$H helix | Yes | +++ | (58; 59) |
| L285Q* | NSCLC | Part of hydrophobic cluster 1 | No | – | (36) |
| R297S | PJS | Ion pair with E223 from the PPE motif (helix $\alpha$EF) | No | – | (44) |
| R297K | PJS | Ion pair with E223 from the PPE motif (helix $\alpha$EF) | No | – | (57) |
| R304W | PJS | Structural role; hydrogen bonds with D162, E165 | No | + | (56) |
| W308C | PJS | Part of hydrophobic cluster 1 | No | – | (47; 60) |
| P314H | PJS | C-terminal flanking tail; binding of possible interactors/substrates | Yes | +++ | (56) |
| P315S* | PJS | C-terminal flanking tail; binding of possible interactors/substrates | Yes | +++ | (55) |
| P324L | PJS | C-terminal flanking tail; binding of possible interactors/substrates | Yes | +++ | (61; 62) |

Comp., Complex formation; Act., LKB1 activity (–, <5%; +, 5-25%; ++, 25-50%; + + +, >50%); PJS, Peutz-Jeghers syndrome; NSCLC, non-small cell lung carcinoma; HNSCC, head and neck non-small cell carcinoma; A-loop, Activation loop; *Mutants tested in this study

# References


1. I. Berger, D. J. Fitzgerald, T. J. Richmond, *Nat Biotechnol* **22**, 1583 (2004).

2. T. S. Walter, *et al.*, *Structure* **14**, 1617 (2006).

3. E. Zeqiraj, *et al.*, *PLoS Biol* **7**, e1000126 (2009).

4. Z. Otwinowski, W. Minor, *Methods in Enzymology* **276**, 307 (1997).

5. A. J. McCoy, *Acta Crystallogr D Biol Crystallogr* **63**, 32 (2007).

6. T. C. Terwilliger, *Methods Enzymol.* **374**, 22 (2003).

7. C. C. Milburn, J. Boudeau, M. Deak, D. R. Alessi, D. M. F. van Aalten, *Nat. Struct. Mol. Biol.* **11**, 193 (2004).

8. R. Bayliss, T. Sardon, I. Vernos, E. Conti, *Mol Cell* **12**, 851 (2003).

9. P. Emsley, K. Cowtan, *Acta Cryst.* **D60**, 2126 (2004).

10. P. D. Adams, *et al.*, *Acta Crystallogr D Biol Crystallogr* **58**, 1948 (2002).

11. G. N. Murshudov, A. A. Vagin, E. J. Dodson, *Acta Cryst.* **D53**, 240 (1997).

12. R. A. Laskowski, M. W. McArthur, D. S. Moss, J. M. Thornton, *J.Appl.Cryst.* **26**, 283 (1993).

13. S. C. Lovell, *et al.*, *Proteins* **50**, 437 (2003).

14. W. L. DeLano, *Abstr.Pap.Am.Chem.Soc.* **228**, 030 (2004).

15. W. Kabsch, C. Sander, *Biopolymers* **22**, 2577 (1983).

16. R. C. Edgar, *Nucleic Acids Res* **32**, 1792 (2004).

17. C. S. Bond, A. W. Schüttelkopf, *Acta Crystallogr D Biol Crystallogr* **65**, 510 (2009).

18. J. M. Lizcano, *et al.*, *EMBO J* **23**, 833 (2004).

19. D. R. Alessi, *et al.*, *Methods Enzymol* **255**, 279 (1995).

20. D. Neumann, A. Woods, D. Carling, T. Wallimann, U. Schlattner, *Protein Expr Purif* **30**, 230 (2003).

21. S. Dale, W. A. Wilson, A. M. Edelman, D. G. Hardie, *FEBS Lett* **361**, 191 (1995).

22. D. R. Knighton, *et al.*, *Science* **253**, 407 (1991).

23. L. N. Johnson, M. E. M. Noble, D. J. Owen, *Cell* **85**, 149 (1996).

24. M. Huse, J. Kuriyan, *Cell* **109** (2002).

25. C. Kim, C. Y. Cheng, S. A. Saldanha, S. S. Taylor, *Cell* **130**, 1032 (2007).

26. A. A. Russo, P. D. Jeffrey, N. P. Pavletich, *Nat. Struct. Biol.* **3**, 696 (1996).

27. X. Zhang, J. Gureasko, K. Shen, P. A. Cole, J. Kuriyan, *Cell* **125**, 1137 (2006).

28. U. Schulze-Gahmen, H. L. D. Bondt, S. H. Kim, *J Med Chem* **39**, 4540 (1996).

29. P. T. C. Wan, *et al.*, *Cell* **116**, 855 (2004).

30. T. Rajakulendran, M. Sahmi, M. Lefrançois, F. Sicheri, M. Therrien, *Nature* **In press** (2009).

31. J. Boudeau, *et al.*, *J. Cell Sci.* **117**, 6365 (2004).

32. N. . Collaborative Computational Project, *Acta Cryst.* **D50**, 760 (1994).

33. J. Boudeau, G. Sapkota, D. R. Alessi, *FEBS Lett.* **546**, 159 (2003).

34. D. R. Alessi, K. Sakamoto, J. R. Bayascas, *Annu. Rev. Biochem.* **75**, 137 (2006).

35. M. Sanchez-Cespedes, *Oncogene.* **26**, 7825 (2007).

36. S. A. Forbes, *et al.*, *Curr Protoc Hum Genet* **Chapter 10**, Unit 10.11 (2008).

37. A. Rowan, *et al.*, *J Invest Dermatol* **112**, 509 (1999).

38. C. Kuragaki, *et al.*, *Lab Invest* **83**, 35 (2003).

39. A. Hemminki, *et al.*, *Nature* **391**, 184 (1998).

40. M. Strazisar, V. Mlakar, T. Rott, D. Glavac, *Cancer Invest* **27**, 407 (2009).

41. S. Olschwang, C. Boisson, G. Thomas, *J. Med. Genet.* **38**, 356 (2001).

42. H. Ji, *et al.*, *Nature* **448**, 807 (2007).

43. A. Ylikorkala, *et al.*, *Hum Mol Genet* **8**, 45 (1999).

44. A. M. Westerman, *et al.*, *Hum. Mutat.* **13**, 476 (1999).

45. S. M. Dong, *et al.*, *Cancer Res* **58**, 3787 (1998).

46. H. Blons, *et al.*, *BMC Med Genomics* **1**, 25 (2008).

47. H. Mehenni, *et al.*, *Am. J. Hum. Genet.* **63**, 1641 (1998).

48. J. P. Koivunen, *et al.*, *Br J Cancer* **99**, 245 (2008).

49. N. Resta, *et al.*, *Hum Mutat* **20**, 78 (2002).

50. E. Avizienyte, *et al.*, *Am J Pathol* **154**, 677 (1999).

51. P. Guldberg, *et al.*, *Oncogene* **18**, 1777 (1999).

52. W. Qiu, F. Schönleben, H. M. Thaker, M. Goggins, G. H. Su, *Oncogene.* **25**, 2937 (2006).

53. S. Matsumoto, *et al.*, *Oncogene* **26**, 5911 (2007).

54. K. A. Yoon, *et al.*, *Br J Cancer* **82**, 1403 (2000).

55. R. J. Scott, *et al.*, *Clin Genet* **62**, 282 (2002).

56. N. Resta, *et al.*, *Cancer Res* **58**, 4799 (1998).

57. L. A. Boardman, *et al.*, *Hum Mutat* **16**, 23 (2000).

58. Y. Nishioka, *et al.*, *Jpn J Cancer Res* **90**, 629 (1999).

59. Z. J. Wang, *et al.*, *J Med Genet* **36**, 365 (1999).

60. R. Onozato, *et al.*, *Cancer Sci* **98**, 1747 (2007).

61. W. S. Park, *et al.*, *Int J Oncol* **13**, 601 (1998).

62. A. M. Westerman, *et al.*, *Lancet* **353**, 1211 (1999).